ФИЗИКА

УДК 536.425:669.017

High-Entropy FeCoCrNiMn and FeCoNiCrAl Alloys Coatings: Structure and Properties*

X. Chen[1, 3], Yu.F. Ivanov[2], V.E. Gromov[3], M.O. Efimov[3], S.V. Konovalov[3], V.V. Shlyarov[3], I.A. Panchenko[3]

[1]Wenzhou University (Wenzhou, China)
[2]Institute of High Current Electronics SB RAS (Tomsk, Russia)
[3]Siberian State Industrial University (Novokuznetsk, Russia)

Покрытия из высокоэнтропийных сплавов FeCoCrNiMn и FeCoNiCrAl: структура и свойства

С. Чень[1, 3], Ю.Ф. Иванов[2], В.Е. Громов[3], М.О. Ефимов[3], С.В. Коновалов[3], В.В. Шляров[3], И.А. Панченко[3]

[1]Университет Вэньчжоу (Вэньчжоу, Китай)
[2]Институт сильноточной электроники СО РАН (Томск, Россия)
[3]Сибирский государственный индустриальный университет (Новокузнецк, Россия)

High-entropy alloys are a new class of materials consisting of at least five elements in an equiatomic or close to equiatomic ratio, which provides them with unique properties. Non-equiatomic high-entropy Fe-Co-Cr-Ni-Mn and Fe-Co-Cr-Ni-Al alloy coatings were applied to the 5083 alloy substrate using wire arc additive manufacturing and the cold metal transfer process. The structure, elemental composition, mechanical and tribological properties of coating / substrate systems were analyzed using modern methods of materials physics. The deposition of FeCoCrNiMn and FeCoNiCrAl HEA coatings on the surface of 5083 alloy was accompanied by the formation of gradients of elemental composition and mechanical properties. A transition layer with a thickness up to 450 μm was formed at the coating / substrate interface located at the coating-substrate boundary. The elemental composition gradient of the transition layer was studied, and a high level of chemical homogeneity of the coating was revealed. Alloying of the coating with substrate elements was observed. The alloying of the substrate with coating elements is accompanied by nonmonotonic changes of element composition in the 500 μm depth layer.

Высокоэнтропийные сплавы — новый класс материалов, состоящих из не менее 5 элементов в эквиатомном или близком к эквиатомному соотношению, что придает им необычные свойства. Покрытия из неэквиатомного высокоэнтропийного сплава Fe-Co-Cr-Ni-Mn и Fe-Co-Cr-Ni-Al были нанесены на подложку из сплава 5083 с использованием технологии проволочно-дугового аддитивного производства и холодного переноса металла. Структура, элементный состав, механические и трибологические свойства систем покрытие / подложка проанализированы с использованием современных методов физического материаловедения. Нанесение покрытий FeCoCrNiMn и FeCoNiCrAl ВЭС на поверхность сплава 5083 сопровождалось формированием градиентов элементного состава и механических свойств. На границе покрытие / подложка сформировался переходный слой толщиной до 450 мкм. Исследован градиент элементного состава переходного слоя и выявлен высокий уровень химической однородности покрытия. Наблюдалось легирование покрытия элементами подложки. Легирование подложки элементами покрытия сопровождается в слое толщиной до 500 мкм немонотонным изменением элементного состава.

* This study is funded by a grant of the Russian Science Foundation, project 23-49-00015. https://rscf.ru/en/project/23-49-00015/

Keywords: FeCoCrNiMn and FeCoNiCrAl high-entropy alloys, coating, 5083 alloy, microhardness, wear resistance, structure.

Ключевые слова: высокоэнтропийные сплавы FeCoCrNiMn и FeCoNiCrAl, покрытие, сплав 5083, микротвердость, износостойкость, состав.

DOI: 10.14258/izvasu(2023)4-01

Introduction

High-entropy alloys (HEAs) were first described at the beginning of the century as alloys containing five and more principal elements with a concentration of each from 5 to 35 % [1–2]. In recent years, there has been an exponential growth of articles devoted to the creation and study of HEA, for example, their number in Elsevier journals has increased almost 100 times [3].

Several reviews have been published [4–8] discussing the most interesting properties of HEAs. In these works, the authors described the thermodynamics of HEAs, the results of their structure modelling, updated methods of producing alloys. HEAs are characterised by high strength and plasticity at high and cryogenic temperatures, corrosion resistance, special magnetic and electrical properties, other functional properties. An attempt was made to analyse recent publications on structure formation, phase composition and properties of predominately five-component alloys MnCoCrFeNi and AlCoCrFeNi as well as fields of their possible application. Excellent mechanical properties of AlCoCrFeNi alloy were studied at different temperatures [9]. The yield strength and strength increased by 29.7 and 19.9 %, as the temperature decreased from 298 to 77 K.

The best known HEA CrMnFeCoNi (Cantor alloy) [8, 10, 11] with a fcc lattice, despite its excellent mechanical properties especially at cryogenic temperatures, impact strength exceeding 200 MPa m^2 and increased creep resistance, are characterised by low strength <400 MPa at room temperature, which makes it necessary to increase it. Significant efforts have been made to solve this problem through grain boundary strengthening [10, 11], solid solution strengthening [12–14], precipitation strengthening [15], and related theoretical developments [16]. Another way to increase strength is partial amorphization, since the amorphous structure does not contain grain boundaries or dislocations [12].

External energy impacts (and, first of all, electron beams) modify the surface layers and significantly improves the functional properties of HEAs [12, 17]. Difficulties in interpreting the strength and plasticity of HEAs are connected with the incomplete understanding of dislocations motion through compositionally misoriented lattices. A quantitative theoretical analysis of mechanical properties (such as work hardening, plasticity, twinning, fracture, fatigue) is difficult for HEAs, since there is even no unambiguous approach for dilute alloys [2].

The last ten years were marked by the attention of scientists to development and study of HEA compounds such as carbides, nitrides, oxides, borides, silicides [17, 18]. The type of lattice of nitride coatings largely depends on the heat and the predominance of nitrides with a certain type of crystal lattice. Single-phase high-entropy nitride coatings are thermally stable [19]. The wire-arc additive manufacturing (WAAM) takes a significant place among the numerous methods of HEAs production [17, 20]. WAAM has a number of advantages in the production of large-sized products. The main attention should be paid to the analysis of structural-phase states and properties of HEA coatings applied to various substrates.

The aim of this work is to analyse the structure and properties of FeCoCrNiMn and FeCoNiCrAl Cantor HEA coatings deposited on 5083 alloy.

Materials and Methods

Samples of the coating/substrate system were used as research materials. The coating was high-entropy alloys of non-equiatomic elemental composition FeCoNiCrAl and FeCoCrNiMn applied to the substrate by the method of wire arc additive technology (WAAM) [17, 20, 21] Modes of FeCoCrNiMn deposition: wire feed speed 8.5 m/min, current ~90 A, voltage 19 V, inductance 1 H, travel speed: initial speed 200 mm/min, final speed 220 mm/min, acceleration 42 mm/min^2, layer length 100 mm, torch inclination angle 10 degrees, surfacing direction "away from oneself" (angle forward). FeCoCrNiAl deposition: wire feed speed 13 m/min, current ~90 A, voltage 22 V, inductance 3 H, travel speed 200 mm/min, layer length 50 mm, torch angle 10 degrees, direction of deposition "away from oneself" (angle forward). The substrate was 5083 aluminium alloy (Table 1). Analysis of the structural-phase states and elemental composition was carried out by transmission electron microscopy and X-ray spectral microanalysis.

Table 1

Chemical composition of 5083 alloy (wt. %)

Cr	Cu	Fe	Mg	Mn	Si	Ti	Zn	Other elements	Al
<0.25	<0.10	<0.40	4.0÷4.9	<1.0	<0.10	<0.15	<0.25	<0.15	Rest

Results and Discussion

Studies of mechanical properties of microhardness profile showed that the microhardness values vary within (2.5–3.5) GPa and increase almost to 9.9 GPa at the boundary with the substrate in the volume of coating composed of high-entropy alloy FeCoCrNiMn. The hardness of the substrate at the boundary with the coating reaches 8 GPa and quickly (at a distance of 300 μm) decreases to 1.1 GPa, almost corresponding to the substrate hardness (1.0 GPa).

For coating composed of high-entropy alloy FeCoNiCrAl, the microhardness values make up ~6.56 GPa and increase to 7.6 GPa at the boundary with the substrate. The hard-ness of substrate near the boundary with coating reaches (1.5–1.6) GPa and decreases to 1.1 GPa at a distance of 5 mm from the boundary. Examination of the longitudinal section of HEA coating (section parallel to the interface coating/substrate) in its middle part showed that the wear coefficient of the coating is $2.3 \cdot 10^{-4}$ mm^3/N·m, and the friction coefficients for FeCoNiCrMn and Fe-CoNiCrAl coatings are 0.7 and 0.24 accordingly.

The results of studying the structure of coating/substrate systems reveal the presence of three layers, namely the coating, the transition layer and the substrate itself. The thickness of transition layer can vary significantly from 100 μm to 450 μm.

Structure and elemental composition of coating composed of FeCoCrNiMn HEA

The study of the coating cross-section revealed the presence of micropores and mi-crocracks. Etching of the coating showed that it can be divided into three sublayers ac-cording to the degree of etching.

The transition layer of the coating/substrate system has a highly developed relief, which indicates that the coating fused into the surface layer of the substrate. A sublayer of acicular structure is located between the transition layer and the substrate (Fig. 1).

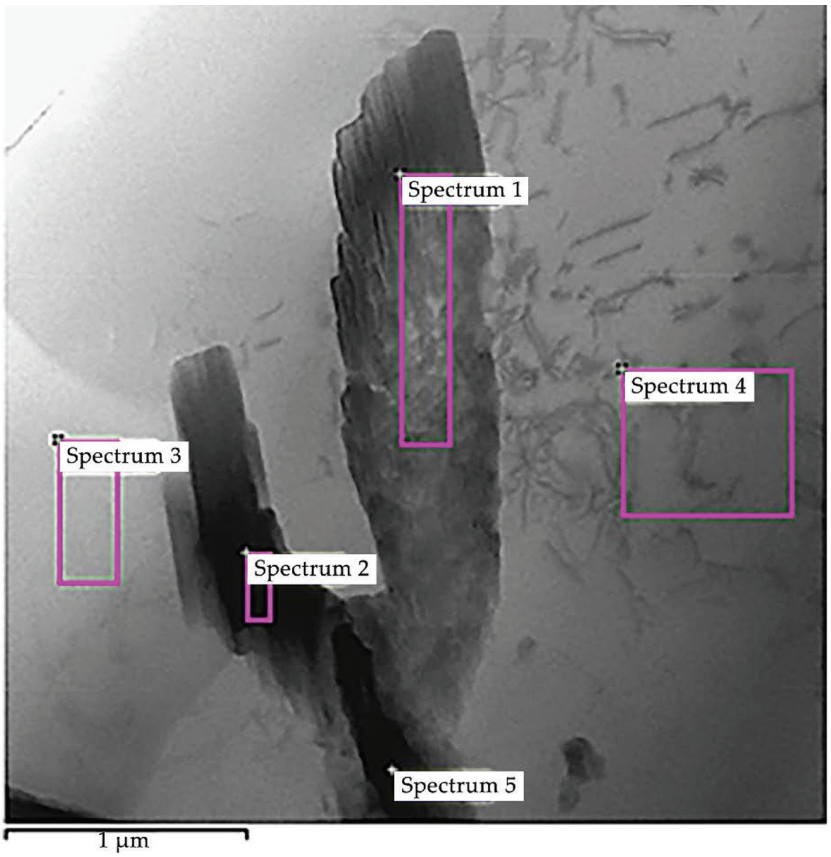

Fig. 1. Electron microscopic image of inclusion located in the contact zone; the areas with the obtained elemental composition are highlighted

X-ray microanalysis of this foil section revealed the following set of chemical elements (at.%): 3.2Mg-93.2Al-0.4Cr-0.6Mn-1.3Fe-1.1Co-0.2Ni. Figure 2 provides an image of the foil section, obtained in the characteristic X-ray radiation of the identified atoms, showing that the inclusion of a lamellar form is located in the structure of aluminium-based alloy and is enriched in Cr, Fe, Mn, Co atoms, i.e. coating-forming atoms (HEA).

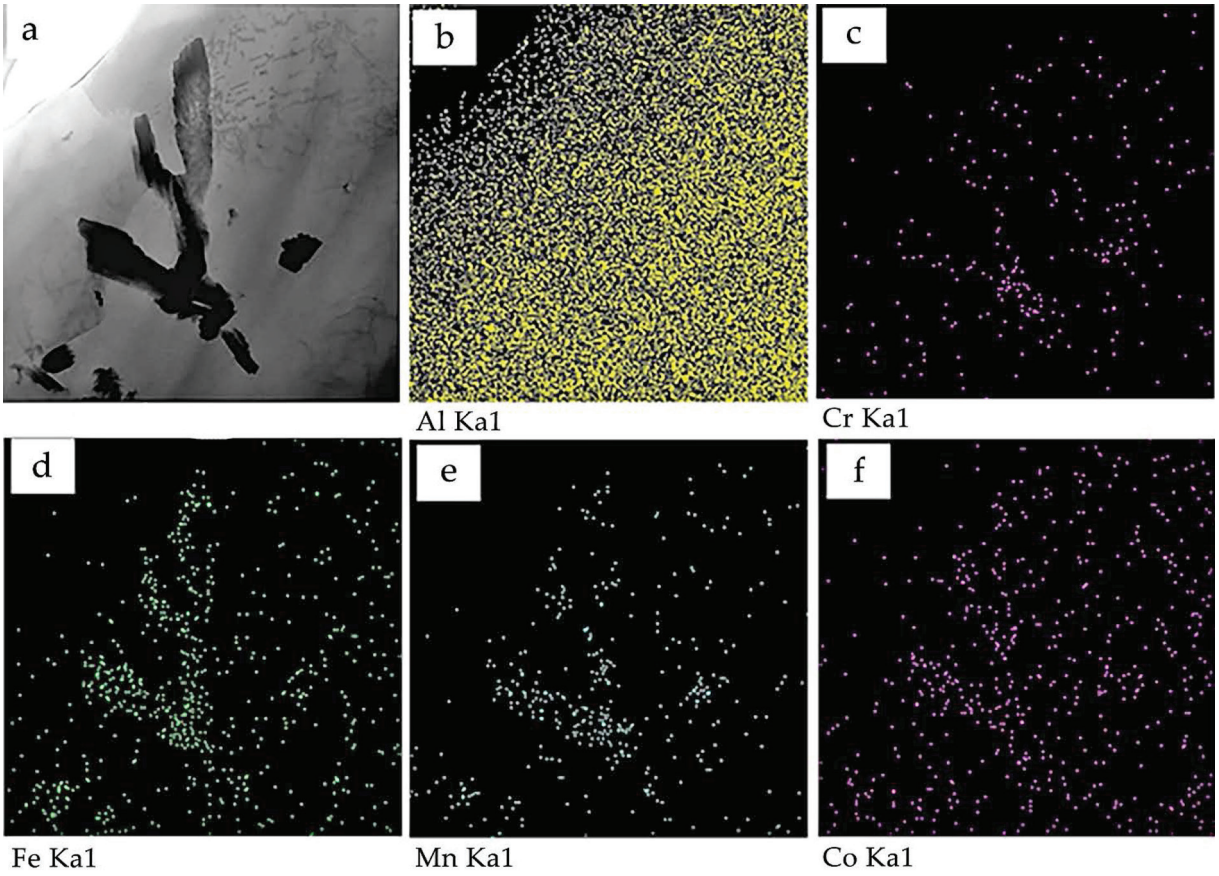

Fig. 2. TEM image of the contact zone structure (a), (b–f) images of the foil section of the obtained as the result of characteristic X-ray radiation of, respectively, Al, Cr, Fe, Mn, Co atoms

Table 2

Elemental composition of the areas of the contact zone indicated in Figure 1

Spectrum	Mg, at.%	Al, at.%	Cr, at.%	Mn, at.%	Fe, at.%	Co, at.%	Ni, at.%
Spectrum 1	4.48	88.56	0.43	1.26	2.92	1.57	0.77
Spectrum 2	0.08	81.25	1.31	3.62	8.84	3.51	1.40
Spectrum 3	5.93	94.07	–	–	–	–	–
Spectrum 4	3.10	96.90	–	–	–	–	–
Spectrum 5	0.95	81.24	1.26	3.59	8.27	3.47	1.22

The analysis of the foil section from the selected areas (Fig. 1) made it possible to define the elemental composition of the inclusion (Table 2). It is clearly seen that the inclusion is enriched in atoms that form HEAs (spectra 1, 2, 5). The inclusion is located in alloy 5083 (spectra 3 and 4). HEA elements in 5083 alloy are not detected.

Microelectron diffraction patterns and dark-field images were used to analyse the phase composition of this foil section (Fig. 3). Indexing of the microelectron diffraction pattern (Fig. 3, b) gives grounds to conclude that this inclusion is iron aluminide $Al_{13}Fe_4$.

Typical electron microscopic images of the HEA structure in the contact zone are shown in Figure 4. A submicrocrystalline grain-subgrain structure is observed with a size of crystallites varying from 0.5 μm to 1.1 μm (Fig. 4, a). The volume of grains contains a dislocation substructure shaped as randomly distributed dislocations or dislocation clusters. A structure typical for the initial stage of the formation of dislocation cells is observed far less frequently (Fig. 4, b). The scalar density of dislocations was determined by random linear intercept method and it approaches $(0.8–1.0)\cdot10^{10}$ cm^{-2}.

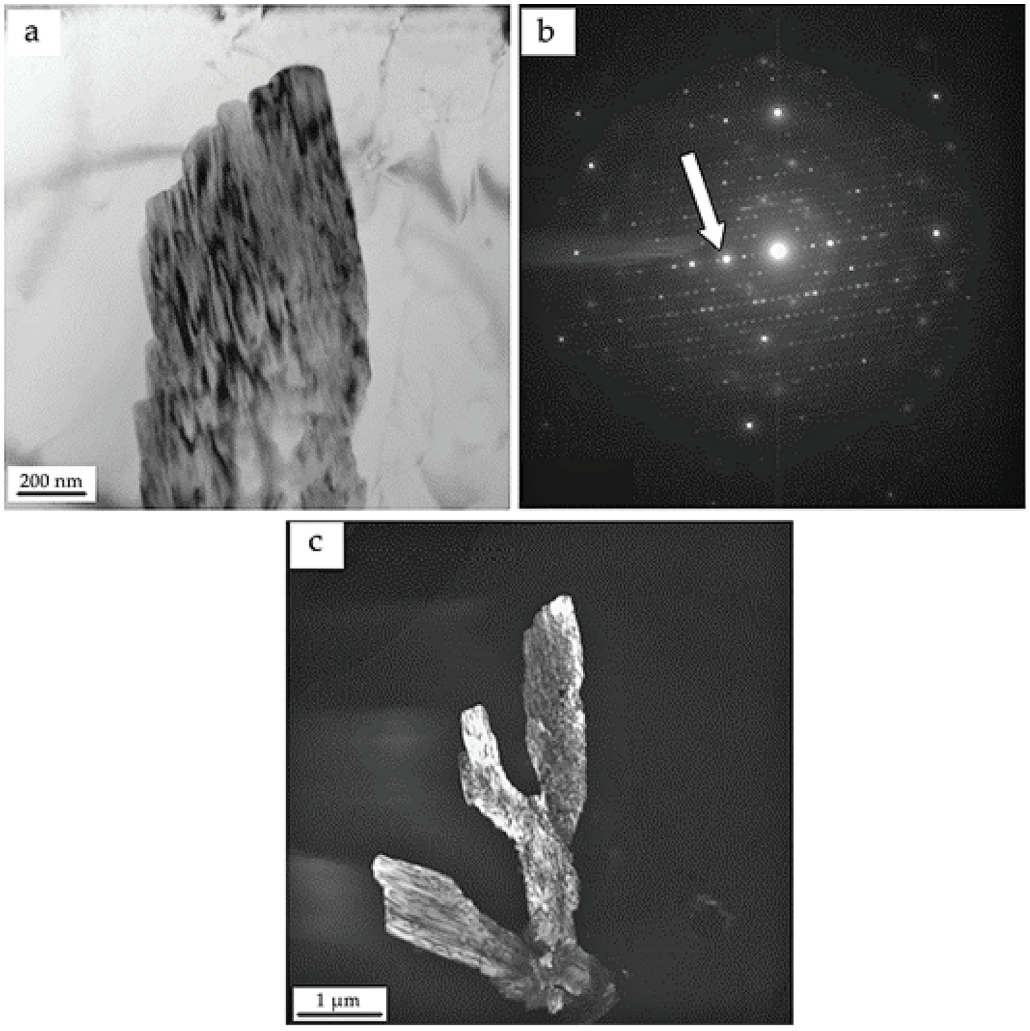

Fig. 3. TEM image of the inclusion located in the contact zone between the coating and the substrate; (a) bright field; (b) microelectron diffraction pattern; (c) dark field obtained in [600] $Al_{13}Fe_4$ reflection; in (b) the arrow indicates the reflection where dark field was obtained

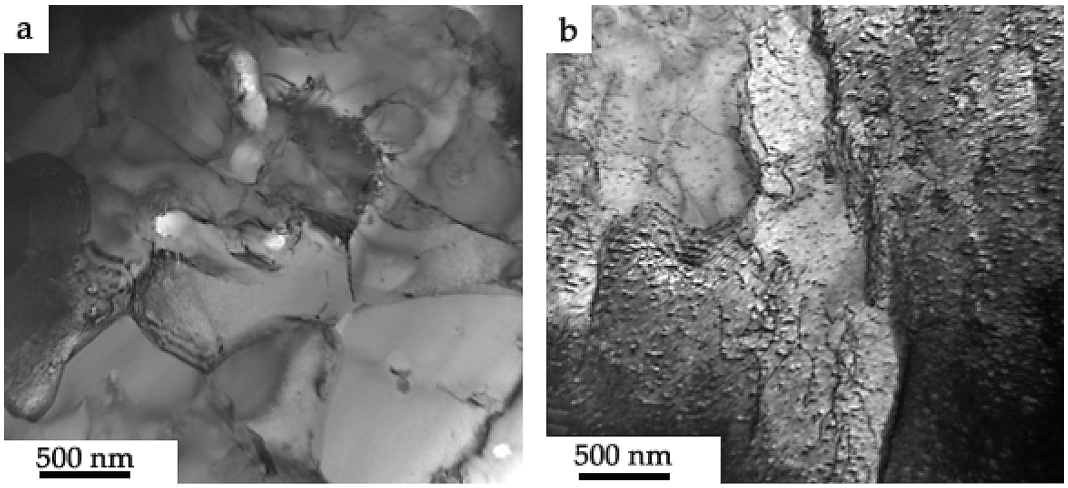

Fig. 4. TEM image of the HEA structure in the contact zone between the coating and the substrate; (a) grain-subgrain structure; (b) cellular dislocation substructure

The phase composition and defective substructure analysis conducted in this work makes it possible to assume about the physical mechanisms of the increase of material hardness in the zone of coating and substrate contact. Namely, (1) strengthening of the substrate is due to the formation of iron aluminides of lamellar morphology; (2) hardening in the high-entropy alloy is a result of the formation of grain-subgrain structure with submicron sizes, at the boundaries and in the volume of which nanosized particles of the second phase are observed; (3) mutual alloying of the substrate and coating indicates solid-solution hardening of the material of the contact zone; (4) the formation of internal stress fields in the contact zone should not be excluded due to the difference in the thermophysical characteristics of the contacting materials.

Structure and elemental composition of coating composed of FeCoCrNiAl HEA

The cross-section of the coating composed of FeCoNiCrAl HEA has a structure typical for a two-phase material, in which inclusions of the second phase are present in the volume of the main phase (Fig. 5). Inclusions of the second phase are rounded (globular) and are located along the grain boundaries of the main phase. The sizes of inclusions of the second phase vary from 2 μm to 9 μm. The microcracks in the coating are also present.

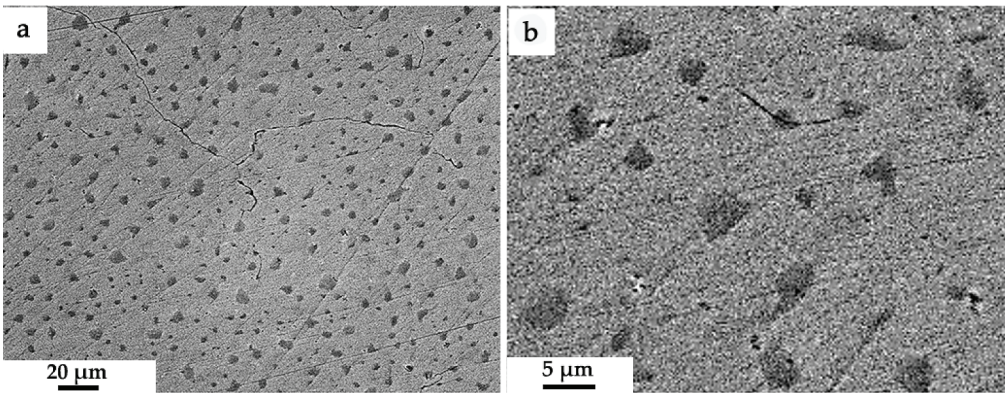

Fig. 5. TEM image of the coating structure, revealed on the cross-section of the coating/substrate system

The substrate layer adjacent to the coating has a lamellar structure as in FeCoCrNiMn HEA. The latter indicates that the substrate is alloyed with chemical elements of the coating followed by phase transformations in the substrate. Obviously, this explains the increase in the microhardness of this substrate layer.

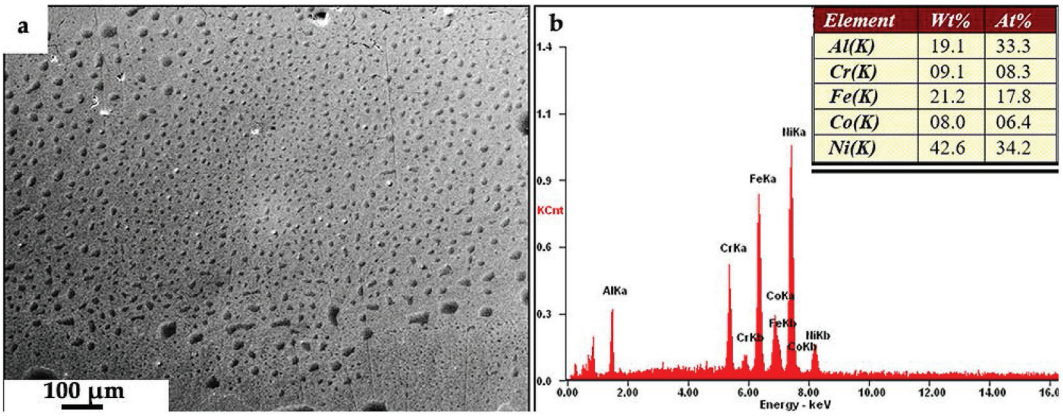

Element	Wt%	At%
Al(K)	19.1	33.3
Cr(K)	09.1	08.3
Fe(K)	21.2	17.8
Co(K)	08.0	06.4
Ni(K)	42.6	34.2

Fig. 6. Structure (a) and energy spectra (b) received from the coating area (a).

Figure 6 shows the results of X-ray spectral microanalysis of the elemental composition in the central part of coating indicating the presence of elements that form HEAs deposited on the substrate. The results of quantitative analysis of coating elemental composition are shown in Table 3.

Table 3

Analysis results of the coating elemental composition, obtained at different distances from the coating surface

X, μm	Elemental composition, at.%				
	Al	Cr	Fe	Co	Ni
100	30.9	11.5	21.9	6.5	29.2
350	30.8	12.3	23.1	6.2	27.6
600	34.8	5.8	15.1	6.1	38.2
900	35.1	7.5	17.5	6.2	33.7

The elemental analysis of the near-boundary layer, the layer of contact between the coating and the substrate was performed (Fig. 7). The results of quantitative analysis of zones 1 and 2 are shown in Table 4.

Table 4

Elemental composition of the adjacent layers of coating and substrate indicated in Figure 7

Scope of analysis	Elemental composition, at.%					
	Mg	Al	Cr	Fe	Co	Ni
1	2.04	32.06	9.55	19.75	6.03	30.56
2	5.92	92.09	0.28	0.57	0.18	0.95

It can be noted that the coating layer with a thickness of at least 100 μm is alloyed with substrate elements and the insignificant penetration of coating elements into the substrate under conditions of low-level contact between the substrate and coating. In this case, the acicular structure is not formed in the substrate (Fig. 7 a).

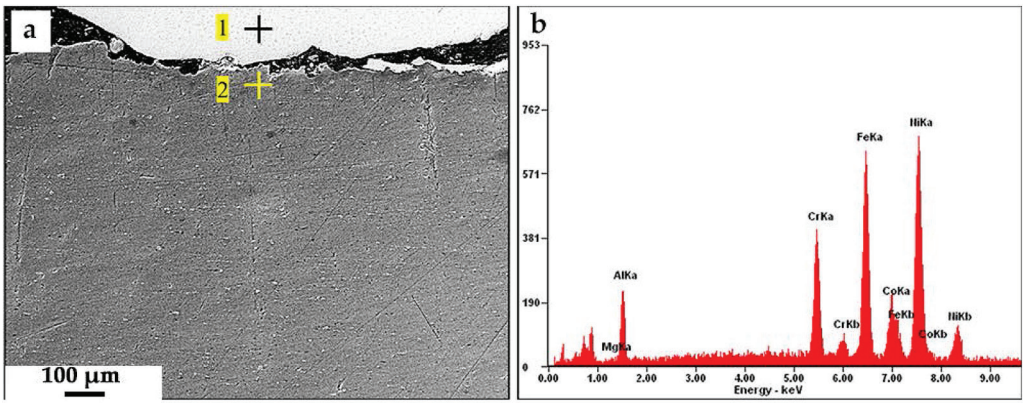

Fig. 7. Structure (a) and energy spectra (b), received from the area indicated by "+" and the number 1 in the coating (a)

An elemental analysis of the substrate layer with acicular structure adjacent to the coating was performed. The example of analysis by the method "by points" is shown in Figure 8.

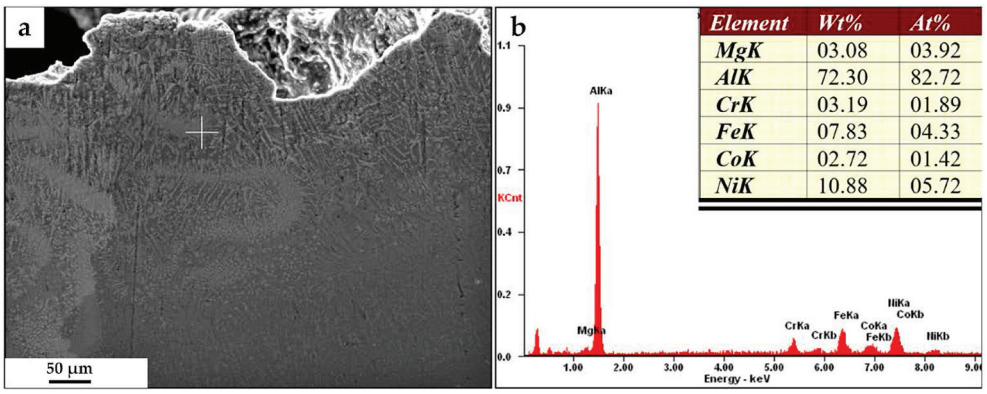

Fig. 8. Structure of the substrate layer adjacent to the coating (a) and energy spectra (b), ob-tained from the point indicated on (a) by "+"

The analysis results of the elemental composition gradient of the substrate layer adjacent to the coating are shown in Figure 9. It is clearly seen that when the fusion of the coating and substrate takes place, the thickness of the alloyed substrate layer reaches 450–500 μm. As for FeCoNiCrMn HEA, the alloying elements are randomly distributed within the substrate thickness. In this case, it is possible to reveal a certain quasi-periodic nature of alloying elements distribution (Fig. 9 b), which is due to the features of coating/substrate formation.

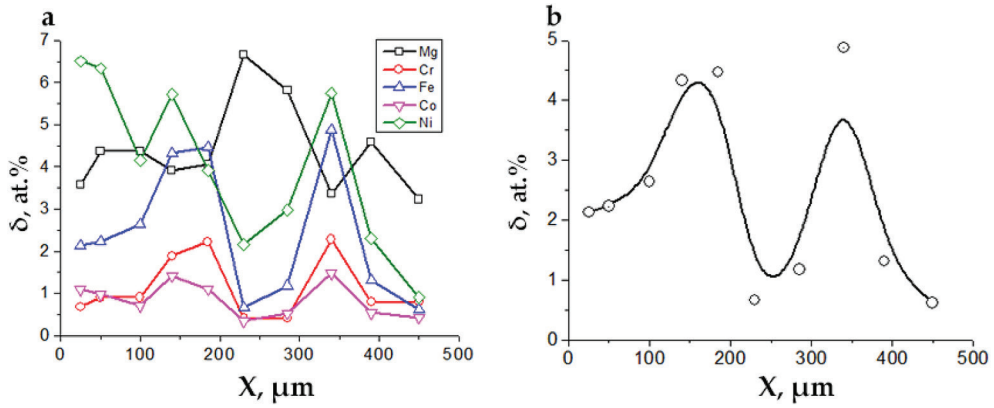

Fig. 9. Dependence of all aluminium-alloying elements (a) and iron concentration (b) on the distance from substratecoating interface (the rest is Al).

Conclusions

The structure, elemental composition, mechanical and tribological properties of coating (HEA)/(alloy 5083) substrate systems formed by cold metal transfer technology were studied using methods of modern materials science.

The following main results were obtained:

— deposition of FeCoNiCrAl and FeCoCrNiMn HEAs on the surface of 5083 alloy was accompanied by the formation of a gradient structure. It was characterised by a natural change in microhardness, elemental and, obviously, phase composition;

— change in the microhardness of coating (HEA)/(alloy 5083) substrate systems had a nonmonotonic character;

— lamellar structure in the layer of substrate adjacent to the coating was formed;

— transition layer up to 450 μm thick was revealed at the coating/substrate interface;

— coating layer adjacent to the substrate was alloyed with substrate elements;

— in a layer up to 500 μm thick, alloying of the substrate with coating elements was accompanied by a nonmonotonic change in the elemental composition of aluminium alloy.

Reference

1. Yeh J.W. Alloy design strategies and future trends in high-entropy alloys // JOM. 2013. Vol. 65. https://doi.org/10.1007/s11837-013-0761-6

2. Yeh J.W. Recent progress in highentropy alloys // Annales de Chimie: Science des Materiaux. 2006. Vol. 31. No. 6. DOI:10.3166/acsm.31.633-648

3. Li Z., Zhao S., Ritchie R.O., Meyers M.A. Mechanical properties of highentropy alloys with emphasis on facecentered cubic alloys // Progress in Materials Science. 2019. Vol. 102. https://doi.org/10.1016/j.pmatsci.2018.12.003

4. Yeh J.W., Chen S.K., Lin S.J., Gan J.Y., Chin T.S., Shun T.T., Tsau C.H., Chang S.Y. Nanostructured high-entropy alloys with multiple principal elements: Novel alloy design concepts and out-comes // Advanced Engineering Materials. 2004. Vol. 6. No. 5. https://doi.org/10.1002/adem.200300567

5. Zhang Y., Yang X., Liaw P.K. Alloy design and properties optimization of high-entropy alloys // JOM. 2012. Vol. 64. No. 7. https://doi.org/10.1007/s11837-012-0366-5

6. Zhang L.S., Ma G.-L., Fu L.-C., Tian J.-Y. Recent progress in high-entropy alloys // Advanced Materials Research. 2013. Vol. 631-632. https://doi.org/10.4028/www.scientific.net/AMR.631-632.227

7. Zhang Y., Zuo T.T., Tang, Z., Gao M.C., Dahmen K.A., Liaw P.K., Lu Z.P. Microstructures and properties of high-entropy alloys // Progress in Mater. Sci. 2014. Vol. 61. https://doi.org/10.1016/j.pmatsci.2013.10.001

8. Gali A., George E.P. Tensile properties of high- and medium-entropy alloys // Intermetallics. 2013. Vol. 39. https://doi.org/10.1016/j.intermet.2013.03.018

9. Qiao J.W., Ma S.G., Huang E.W., Chuang C.P., Liaw P.K., Zhang Y. Microstructural characteristics and mechanical behaviors of AlCoCrFeNi high-entropy alloys at ambient and cryogenic temperature // Materials Science Forum. 2011. Vol. 688. https://doi.org/10.4028/www.scientific.net/MSF.688.419

10. Wu Z., Bei H., Pharr G.M., George E.P. Temperature dependence of the mechanical properties of equiatomic solid solution alloys with face-centered cubic crystal structures // Acta Materialia. 2014. Vol. 81. https://doi.org/10.1016/j.actamat.2014.08.026

11. Schuh B., MendezMartin F., Völker B., George E.P., Clemens H., Pippan R., Hohenwarter A. Mechanical properties, microstructure and thermal stability of a nanocrystalline CoCrFeMnNi highentropy alloy after severe plastic deformation // Acta Materialia. 2015. Vol. 96. https://doi.org/10.1016/j.actamat.2015.06.025

12. Li Z., Tasan C.C., Springer H., Gault B., Raabe D. Interstitial atoms enable joint twinning and transformation induced plasticity in strong and ductile highentropy alloys // Scientific Reports. 2017. Vol. 7. https://doi.org/10.1038/srep40704

13. Xiao L.L., Zheng Z.Q., Guo S.W., Huang P., Wang F. Ultra-strong nanostructured CrMnFeCoNi high entropy alloys // Materials and Design. 2020. Vol. 194. https://doi.org/10.1016/j.matdes.2020.108895

14. Coury F.G., Kaufman M., Clarke A.J. Solid-solution strengthening in refractory high entropy alloys // Acta Materialia. 2019. Vol. 175. https://doi.org/10.1016/j.actamat.2019.06.006

15. Ikeda Y., Tanaka I., Neugebauer J., Körmann F. Impact of interstitial C on phase stability and stackingfault energy of the CrMnFeCoNi highentropy alloy // Physical Review Materials. 2019. Vol. 3. No. 11. https://doi.org/10.1103/PhysRevMaterials.3.113603

16. Laplanche G., Kostka A., Horst O.M., Eggeler G., George E.P. Microstructure evolution and critical stress for twinning in the CrMnFeCoNi highentropy alloy // Acta Materialia. 2016. Vol. 118. https://doi.org/10.1016/j.actamat.2016.07.038

17. Gromov V.E., Konovalov S.V., Ivanov Yu.F., Osintsev K.A. Structure and properties of high entropy alloys. Springer, 2021.

18. Pogrebnyak A.D., Bagdasaryan A.A., Yakushchenko I.V., Beresnev V.M. Structure and properties of high-entropy alloys and nitride coatings based on them // Russian Chemical Reviews. 2014. Vol. 83. No. 11. https://doi.org/10.1070/RCR4407

19. Firstov S.A., Gorban V.F., Andreev A.O., Krapivka N.A. Superhard coatings from high-entropy alloys // Science and innovations. 2013. Vol. 9. No. 5.

20. Osintsev K.A., Konovalov S.V., Gromov V.E., Panchenko I.A., Ivanov Yu.F. Microstructural and mechanical characterisation of non-equiatomic Al2.1Co0.3Cr0.5FeNi2.1 high-entropy alloy fabricated via wire-arc additive manufacturing // Philosophical Magazine Letters. 2021. Vol. 101. No. 9. https://doi.org/10.1080/09500839.2021.1936257

21. Osintsev K.A., Konovalov S.V., Glezer A.M., Gromov V.E., Ivanov Y.F., Panchenko I.A., Sundeev R.V. Research on the structure of Al2.1Co0.3Cr0.5FeNi2.1 high-entropy alloy at submicro- and nano-scale levels // Materials Letters. 2021. Vol. 294. https://doi.org/10.1016/j.matlet.2021.129717